Int. J. Electrochem. Sci., 9 **(2014)** xx - yy

International Journal of
ELECTROCHEMICAL SCIENCE
www.electrochemsci.org

γ-Fe_2O_3 Magnetic Core Functionalized with Tetraethyl Orthosilicate and 3-Aminopropyl Triethoxysilane for an Isolation of H7N7 Influenza Serotype Virions

Zbynek Heger[1,2], Natalia Cernei[1,2], Roman Guran[1,2],Petr Michalek[1,2], Vedran Milosavljevic[1,2], Pavel Kopel[1,2], Ondrej Zitka[1,2], Jindrich Kynicky[3], Petr Lany[4], Vojtech Adam[1,2], Rene Kizek[1,2]*

[1] Department of Chemistry and Biochemistry, Faculty of Agronomy, Mendel University in Brno, Zemedelska 1, CZ-613 00 Brno, Czech Republic, European Union
[2] Central European Institute of Technology, Brno University of Technology, Technicka 3058/10, CZ-616 00 Brno, Czech Republic, European Union
[3]Karel Englis College, Sujanovo nam. 356/1, CZ-602 00, Brno, Czech Republic, European Union
[4]Department of Infectious Diseases and Epidemiology, Faculty of Veterinary Medicine, University of Veterinary and Pharmaceutical Science, Palackeho nam. 2, 620 00, Brno, Czech Republic, European Union

[*]E-mail: kizek@sci.muni.cz

Received: / Accepted: / Published:

The influenza viruses cause annual epidemics of respiratory disease and occasional pandemics, which constitute a major public-health issue. The most important tool in the diagnosis of influenza pandemic is timely and right diagnosis. Hence, this study presents synthesis of paramagnetic particles formed by nanomaghemite (γ-Fe_2O_3) core, whose surface was functionalized with tetraethyl orthosilicate (TEOS) and 3-aminopropyl triethoxysilane (APTES), able to bind H7N7 influenza virions. Paramagnetic particles show the ability to immobilize virions for direct analysis using ion-exchange chromatography with VIS detection. The presence of H7N7 virions on surface of paramagnetic beads was confirmed by matrix-assisted laser desorption/ionization time of flight mass spectrometry, based upon the mass weight of H7N7 virions, determined before and after establishment of binding. Moreover, using scanning electrochemical microscopy revealed, that binding is provided due to strong charge-charge interaction between positively charged influenza surface protein hemagglutinin and negatively charged surface of nanocomposite. It can be concluded that paramagnetic beads show significant binding capability towards H7N7 virions.

Keywords: H7N7; Functionalization; Lab-on-a-Chip; Magnetic immobilization; Sensor

1. INTRODUCTION

Influenza virus belongs to the most dangerous infectious agents killed more people in the 20th century than any other virus [1]. In 1918, an influenza A pandemic, notorious known as the "Spanish Flu", caused 50 million deaths worldwide [2] and it is recorded as one of the most devastating epidemics in history. Despite years of research of influenza, this highly contagious disease still continues to kill millions of people of all ages every year. Hence the development of strategies, which can be used to prevent the future expansions of this virus, is an important endeavour.

A variety of technologies for influenza diagnostics has been developed, including *in vitro* virus isolation by culture [3], serologic assays [4], enzyme-linked immunosorbent assay (ELISA) [5], or polymerase chain reaction (PCR)-based assays [6]. However, there still exist disadvantages making these methods complicated for practical applications. *In vitro* cultivation is tedious and time consuming usually lasting 5–7 days [7,8]. PCR is very sensitive to target molecule, but also to undesired, external contamination of the template nucleic acid, and thus may provide false positive results. Serological methods require seroconversion and therefore are not able to detect acute infections [9]. Moreover, there are many issues with virus isolation, requiring trained laboratory workers and a highly sterile environment.

Possibility of rapid, cheap, screening, and diagnostic method may be offered by sensor constructed as a part of the measuring device that converts the input signal to the quantity suitable for the interpretation. The most common sensors utilized for influenza detection are based on various types of electrochemical sensing [10,11]. Because of the fact that sensors may serve as the easy-to-use, simple and sensitive diagnostic tools [12], paramagnetic particles (PMPs) may enhance the mentioned properties of a sensor device. Their advantageous characteristics as small size and high surface area enhance kinetics and provide possibility of manipulation under the influence of an external magnetic field [13,14]. Moreover, due to a possibility of surface functionalization with various chemically-active groups, the isolation process can be performed directly in samples eliminating the sample pre-treatment steps as centrifugation or filtration [15].

In these perspectives, we aimed to suggest and synthesize paramagnetic particles composed of nanomaghemite core with surface modified with various chemical substances. Herein we report that composites prepared by us are able to bind H7N7 influenza serotype virions, and thus they may enhance the simplification, selectivity and sensitivity of an influenza sensor as well as to improve the basic laboratory diagnostic as a preconcentration tool.

2. EXPERIMENTAL PART

2.1. Chemicals and pH measurement

Working solutions like buffers and standard solutions were prepared daily by diluting the stock solutions. Standards and other chemicals were purchased from Sigma-Aldrich (St. Louis, MO, USA) meeting the specification of American Chemical Society (ACS), unless noted otherwise. Methyl cellosolve and tin chloride were purchased from Ingos (Prague, Czech Republic).

2.2. Isolation of H7N7 influenza subtype using sucrose gradient

Chicken embryo in age of 9 days was treated with H7N7 virions and incubated for 48 hours at 37 °C. After proper incubation, allantoic fluid was collected and centrifuged for 30 minutes at 4000 g using Microcentrifuge 5417R (Eppendorf AG, Hamburg, Germany). Supernatant was removed and further centrifuged for 2 hours at 20 000 g. Pellet was resuspended in 1000 μL of phosphate buffered saline (PBS) and stored at 4 °C. For isolation of H7N7 virions, the discontinuous sucrose gradient was employed according to de Jonge and co-workers [16]. Recovery of virions was carried out by removing of virions into PBS and subsequent purification of virions via centrifugation under the following conditions: 30 min, 20 000 g. Resulting sediment was resuspended in 2 mL of PBS with addition of 0.1% sodium azide (*w*/*w*).

2.3. Preparation of nanomaghemite particles

Nanometric maghemite nanoparticles were prepared by dissolving of 7.48 g of iron(III) nitrate nonahydrate ($Fe(NO_3)_3 \bullet 9H_2O$) in 400 mL of water. Reduction was carried out by addition of 1 g $NaBH_4$ in 50 mL of 3.5 % NH_3 (*w*/*v*). Resulting mixture was warmed at 100 ºC for 2 hours. After cooling the mixture was washed with water using for separation a force of external magnetic field.

2.4. Preparation of nanoparticles with different functionalization

MAN 38: 25 mL of isopropanol was added to nanomaghemite and mixture was shaken. Tetraethyl orthosilicate (TEOS) was applied to modify the nanomaghemite surface. Firstly 20 mL of 28% ammonium (*w*/*v*) was mixed with nanomaghemite and subsequently 3.33 mL of TEOS was added. The resulting mixture was stirred at Biosan OS-10 (Biosan, Riga, Latvia) for 2 hours at 40 ºC. Finally 3.33 mL of 3-aminopropyl triethoxysilan (APTES) was added and mixture was warmed for another hour. Resulting product was separated using external magnet and washed with ethanol.

2.5. Scanning electron microscopy

Morphology of paramagnetic particles was revealed using scanning electron microscopy (SEM) FEG–SEM MIRA (Tescan, Brno, Czech Republic). The SEM was fitted with Everhart–Thronley type of SE detector, high speed YAG scintillator based BSE detector, panchromatic CL Detector, and EDX spectrometer. Prior to analyses, the samples were coated by 10 nm of carbon to prevent sample charging. A carbon coater K950X (Quorum Technologies, Grinstead, United Kingdom) was employed. Different conditions were optimized in order to reach either minimum analysis time or maximum detail during an overnight automated analysis. An accelerating voltage of 15 kV and beam currents about 1 nA was applied regarding to maximum throughput.

2.6. X-ray fluorescence analysis of elemental composition

X-ray fluorescence (XRF) analysis was carried out on Xepos (SPECTRO analytical instruments GmbH, Kleve, Germany) fitted with three detectors: Barkla scatter – aluminium oxide, Barkla scatter – HOPG and Compton/secondary molybdenum respectively. Analyses were conducted in Turbo Quant cuvette method of measuring. The experimental parameters were set to – measurement

duration: 300 seconds, tube voltage from 24.81 to 47.72 kV, tube current from 0.55 to 1.0 mA and vacuum switched off.

2.7. GC organic elemental analysis

To obtain the basic information about paramagnetic nanoparticles organic element composition, liquid sample of the nanoparticles was dried at 220 °C, and analysed using Automatic elemental analyser Flash 2000 (Thermo Fisher Scientific, Waltham, MA, USA), equipped with two isothermal GC separation columns (CHN/NC separation columns, 2 m, 6 × 5 mm Stainless, PQS, 2 mm unions, OEA Laboratories Limited, Callington, United Kingdom) and thermal conductivity detector (TCD). The flow rate of helium was set to 140 $mL.min^{-1}$, and the separation temperature was set to 65 °C.

2.8. Ion-exchange chromatography

For the identification of paramagnetic particles binding capacity the ion-exchange liquid chromatography with post column derivatization by ninhydrin was used and the absorbance detector in the VIS range set to 440 nm was employed. Glass column, tempered to 60 °C with inner diameter of 3.7 mm and 350 mm length was filled manually with strong cation exchanger in sodium cycle LG ANB with approximately 12 μm particles and 8% porosity. Experimental conditions were applied according to our preliminary study [17].

2.9. Matrix-assisted laser desorption/ionization time of flight mass spectrometry

Matrix-assisted laser desorption/ionization time of flight (MALDI-TOF/TOF) mass spectrometry (Bruker, Billerica, MA, USA) was employed to confirm a presence of virion after binding to paramagnetic particles. 2,5-dihydroxybenzoic acid was used as the matrix (Sigma-Aldrich). The saturated matrix solution was prepared in 50% methanol (*v*/*v*) and 0.1% trifluoroacetic acid (*v*/*v*). Mixture was vortexed and ultrasonicated using Bandelin 152 Sonorex Digital 10P ultrasonic bath (Bandelin electronic GmbH, Germany) for 2 minutes at 50 % intensity at room temperature. A dried-droplet method was used for sample preparation. The sample solution was mixed with matrix solution in volume ratio 1:1. After obtaining a homogeneous solution, 2 μL of mixture was applied on the target plate and dried under atmospheric pressure at room temperature. All measurements were performed in the linear positive mode in the m/z range 1-20 kDa. The mass spectra were acquired by averaging 2500 subspectra from a total of 2500 shots of the laser. Laser power was set 5-10 % above the threshold.

2.10. Scanning electrochemical microscope for characterization of paramagnetic particles

The measurement of cyclic voltammograms as well as relative current response before and after H7N7 binding to PMPs was detected by scanning electrochemical microscope Model 920D (CH instruments, Inc. USA). Electrochemical microscope consisted of 10 mm measuring platinum disc probe electrode with potential of 0.2 V. Another platinum disc electrode with O-ring as conducting substrate used potential of 0.3 V. During scanning, the particles were attached on the substrate platinum electrode by magnetic force from neodyme magnet, which was situated below the electrode. Platinum measuring electrode was moving from 150 μm above the surface. The scanning was carried

out in the solution consisting of 5% ferrocene in methanol mixed in ratio 1:1 (*v*/*v*) with 0.05% KCl in water (*v*/*v*). Measurements were performed in teflon cell with volume of 1.5 mL according to the following parameters: amperometric mode, vertical scan was carried out in area 500 × 500 μm with scan rate of 30 $\mu m.s^{-1}$. Cyclic voltammograms were measured under the following conditions: fixed potential window of -0.2 to 0.5 V; scan rate 0.02 $V.s^{-1}$; number of segments 4; quiet time before individual analysis 10 s; sensitivity 1 nA.

3. RESULTS AND DISCUSSION

To demonstrate the binding ability of various paramagnetic particles prepared by us, we selected H7N7 influenza serotype, also known as the equine influenza. The H7N7 belongs to a subtype of influenza A viruses, which also includes H1N1 responsible for Spanish flu [2] or Swine flu [18], H5N1, which caused Avian flu [19]. These are the most virulent human pathogens among the three influenza subtypes and cause the most severe disease. H7N7 serotype was chosen because of its ideal properties as no zoonotic potential [20] and larger stability in comparison with human influenza subtypes, however, it shows very low resistance to UV light, detergents and disinfectants customarily used in laboratory [21].

3.1. Paramagnetic particles synthesis

Purpose of our study was to suggest and synthesize the paramagnetic particles able to establish a binding with H7N7 influenza serotype, and thus to isolate and immobilize the virions for subsequent analyses. As a primary platform for modification surface active nanometric maghemite particles were chosen. Nanomaghemite acts as an excellent superparamagnetic carrier due to its well defined stoichiometric structure, single-phase character, and quite uniform size distribution with ability to be simply functionalized with various chemically-active groups [22,23]. For nanometric maghemite particles functionalization, substances with potential to cover the nanomaghemite surface and provide active binding sites for H7N7 virions were selected, as it is mentioned in chapter *Experimental Section*, where the entire synthesis procedures are described. The surface coating is crucial for enhancement of the nanoparticles properties, because it can regulate their stability, solubility, and in particular their selectivity [24-26].

3.2. Workflow process resulting in binding of H7N7 virions onto PMPs surface

Firstly, we decided to evaluate a binding capacity of all our synthesized paramagnetic particles. Overall workflow process scheme can be seen in Fig. 1A. Before PMPs application, it was necessary to include three washing steps with phosphate buffered saline (PBS), to remove the undesired impurities, contained in the solid PMPs after synthesis. Further, to achieve the highest yields of H7N7 virions binding onto surface of PMPs, the incubation was carried out according to our previous study, dealing with the isolation of amino acids [17]. After proper incubation, the solution containing unbound virion particles was removed using the force of external magnetic field provided by the permanent magnet (Chemagen, Baesweiler, Germany). Remaining solid PMPs with isolated virions were dissolved in 3 M HCl after application of additional three washing step using PBS (pH 7.4). Subsequently, dissolved PMPs were prepared for the evaporation by nitrogen blow-down evaporator Ultravap 96 with spiral needles (Porvair Sciences limited, Leatherhead, United Kingdom). Evaporated

analyte was finally resuspended with dilution buffer and for screening of paramagnetic particles prepared in different manner ion-exchange chromatography (IEC) was employed.

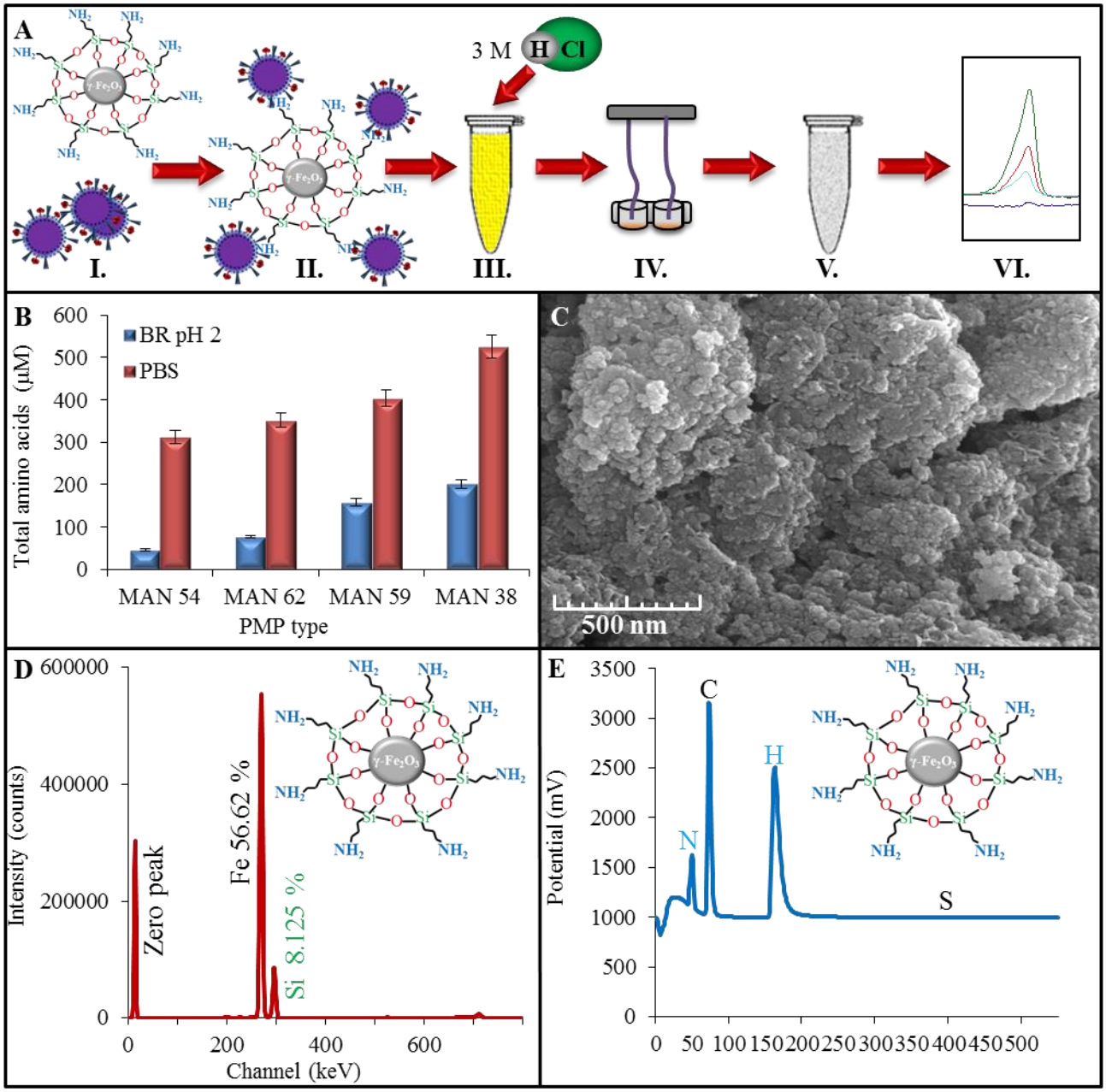

Figure 1. (**A**) Scheme of workflow process, providing the binding between paramagnetic particles (PMPs) and H7N7 influenza virions. Firstly the paramagnetic beads are mixed with influenza virions (**I.**). As a second step incubation is included (**II.**), following by washing step (three times washing with PBS buffer). This process resulted in obtaining of paramagnetic beads with virions on their surface. For characterization of binding capacity of various microparticles H7N7@PMPs conjugate was dissolved in 3 M HCl (**III.**). Further evaporation was carried out (**IV.**) and subsequently dilution buffer was applied for resuspendation of sample (**V.**). Sample prepared in this way was prepared to be analysed using ion-exchange chromatography (IEC). (**B**) IEC was employed for optimization of washing conditions, where application of acidic Britton-Robinson buffer (pH 2) and phosphate buffered saline (PBS, neutral pH) were tested. (**C**) Micrograph of paramagnetic microparticles showing their nanoscaled morphology (Scale

500 nm). (**D**) X-ray fluorescence results providing information about elemental composition of MAN 38. (**E**) C, N, H and S gas chromatographic with TCD determination in the synthesized and modified nanoparticles.

3.3. Screening of binding capacity of various PMPs using IEC

For washing of PMPs in preliminary experiments, Britton-Robinson buffer with pH 2 was tested. Although we observed binding of some analyte onto paramagnetic particles (Fig. 1B), we further attempted to use only PBS for washing and resulting yields were much larger than in acidic pH (comparing 201.4 μM of total amino acids in B-R buffer with 525.7 μM of total amino acids in PBS in the case of MAN 38; 158.3 μM of total amino acids in B-R buffer with 404 μM of total amino acids in PBS in the case of MAN 59; 76.8 μM of total amino acids in B-R buffer with 351.8 μM of total amino acids in PBS in the case of MAN 62; 46.3 μM of total amino acids in B-R buffer with 312.8 μM of total amino acids in PBS in the case of MAN 54). Subsequent elevation of pH was shown not having any significant influence on the analyte yields (data not shown). Previously it was shown that influenza surface proteins hemagglutinin (HA) and neuraminidase (NA) degrade under low pH, which change their conformations leading to the losing their stability [27-29]. Due to this reason we hypothesized that residues of B-R buffer with pH 2 used in washing process may change the spatial properties of H7N7 surface proteins and thus the binding moieties may be made inaccessible for functional groups localized on a surface of PMPs. This resulted in lower yields when compared with neutral pH.

3.4. Morphological characterization

To reveal the particles morphology and to obtain more detailed insight into basic characteristics of paramagnetic particles, which were evaluated as the platform for influenza isolation with the highest yields – MAN 38, scanning electron microscopy (SEM) was employed (Fig. 1C). SEM is a powerful tool applicable in characterization of the surface morphology of different materials including PMPs. As it is shown in Fig. 1C, paramagnetic particles synthesized by us are irregularly shaped, nanoscaled composite, formed by nanomaghemite particles covered by substances used for functionalization (TEOS and APTES in the case of MAN 38). It clearly follows from the results obtained that PMPs form clusters very willingly, but this phenomenon may be caused artificially by sample pre-treatment before SEM analysis in the form of carbon coating. Although, functionalization was carried out, good superparamagnetic ability of composite was retained importantly for immobilization.

3.5. Characterization of elemental composition of PMPs

The following morphological characterization, elemental composition of MAN 38 composite was determined using X-ray fluorescence (XRF) and gas chromatography with thermal conductivity detector (TCD). As it is shown in Fig. 1D, expressing percentage representation of elements forming paramagnetic particles MAN 38, iron (Fe) was identified as the most abundant element with 56.62 % of total content. High proportion of iron is beneficial, because iron forms the main part of nanomaghemite core providing superparamagnetic properties to a composite. As the second most abundant element, silicon (Si) was determined with 8.125 % from total content. Silicon was detected during both functionalization steps as (i) silanization with tetraethyl orthosilicate (TEOS) to form a silica outer shell and (ii) aminopropylation with 3-aminopropyl triethoxysilan (APTES) to add a

coating forming extra aminopropylsilane functional groups [30]. Due to the fact that XRF can determine mainly metal elements, to obtain the information about other elements, as organic building blocks (C, N, H, S) gas chromatography with TCD was employed (Fig. 1E). In compliance with XRF analysis, the increased amount of nitrogen (N) and hydrogen (H), forming the MAN 38 composite´s functional groups, were determined using GC-TCD.

3.6. Confirmation of H7N7 presence on the composite´s surface using MALDI-TOF/TOF MS

To confirm the H7N7 virions presence on paramagnetic particles MALDI-TOF/TOF mass spectrometry was employed. The MALDI mass spectra recorded for the H7N7 virions, as well as for composite are shown in Fig. 2. Virions were directly applied on the target plate after isolation by sucrose gradient and mixed in ratio 1:1 with DHB matrix. Using a linear positive mode with laser power of 80 %, mass-to-charge ratio (m/z) of H7N7 virion was evaluated as approximately 8985. Subsequently, the mass spec analysis of MAN 38 was carried out showing no signal in region, where H7N7 was determined. Finally, the analysis of H7N7 virions bound on the surface of MAN 38 composite was performed. Obtained results (one spectrum as an average from 2500 subspectra) show that H7N7 virions are, after isolation in accordance to our protocol, present on the paramagnetic particles. Mass-to-charge ratio (m/z) was determined as very similar to analysis of virions without PMPs. These results serve as evidence that virions willingly bind onto surface of composite.

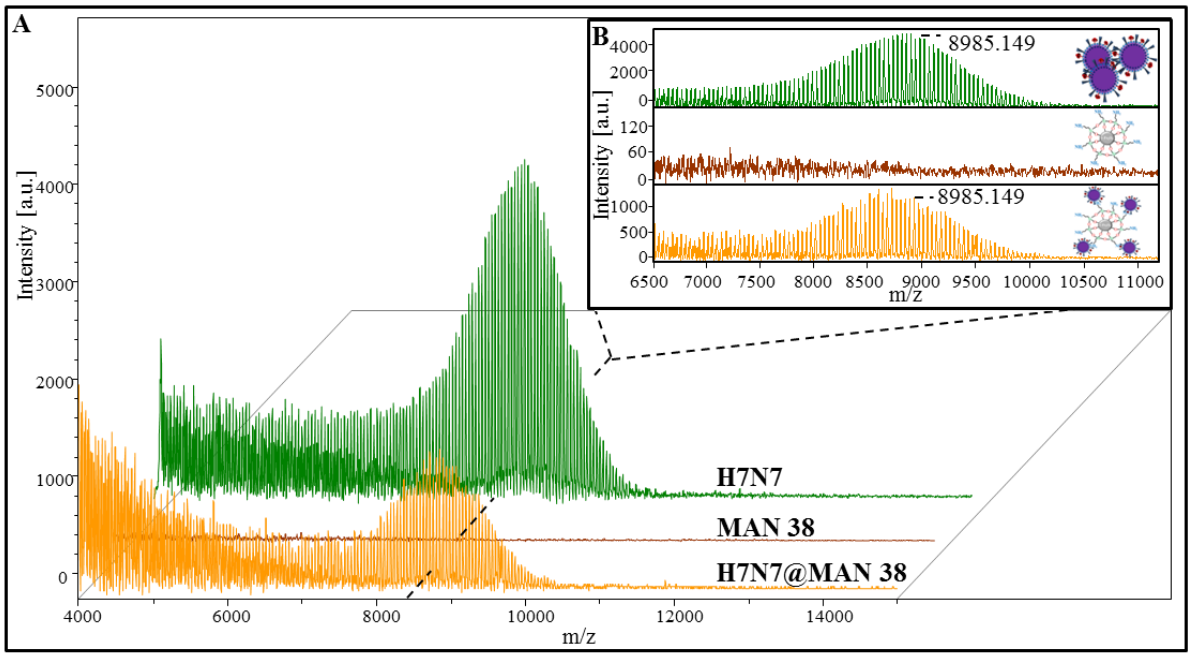

Figure 2. (**A**) MALDI-TOF/TOF mass spectra of H7N7 virions expressed with the green colour, MAN 38 paramagnetic particles expressed with the red colour and H7N7 virions bound at surface of MAN 38 paramagnetic microparticles expressed with the orange colour. (**B**) Zooming of peaks of determined analytes in the same colours as before, showing the same similarity in mass of H7N7 before and after binding at PMPs. Measurements were carried out in DHB matrix, in linear positive mode with laser power of 80 %. One spectrum is made as an average from 2500 subspectra.

3.7. Electrochemical confirmation of H7N7 presence on the composite´s surface

To detect H7N7 virions electrochemistry was carried out. Electrochemical methods have traditionally received the major share of the attention in biosensor development for its advantages such as high sensitivity, specificity and simplicity, and inherent miniaturization of modern electrical bioassays permits them to rival the most advanced optical protocols [31]. Hence, scanning electrochemical microscopy (SECM) was employed to perform cyclic voltammetry experiments to obtain a further insight into electrochemical behaviour of virions and composite using fixed potential window of -0.2 to 0.5 V and scan rate of 0.02 $V.s^{-1}$. As it is obvious, the electrochemical behaviour of paramagnetic particles is markedly influenced by the presence of H7N7 virions (Fig. 3A). This resulted in reduction of signals in both anodic (-0.1 to 0.2 V) and cathodic (0.1 to 0.4 V) potential sweeps.

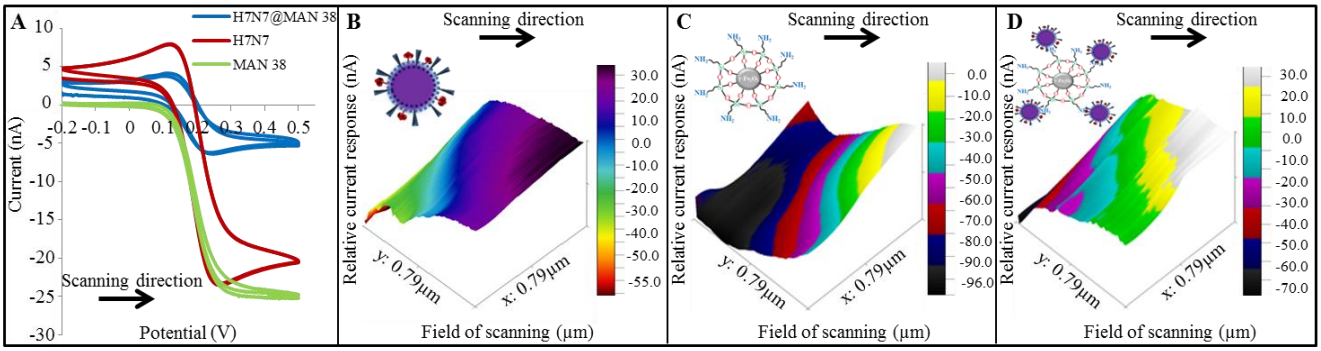

Figure 3. (**A**) Cyclic voltammograms of H7N7 virions, MAN 38 paramagnetic particles and their conjugate. Scanning electrochemical microscope (SECM) was employed to obtain information about relative current response (nA) of PMPs surface. SECM 3D expression of relative current response of (**B**) layer of H7N7 virions, (**C**) bare paramagnetic microparticles MAN 38, and (**D**) paramagnetic microparticles after establishment of binding with H7N7 virions.

Further, SECM was employed to reveal the relative current response on a surface of paramagnetic particles. This approach is very helpful for characterization of the binding of virions to the surface of the particles because of possibility to monitor the electrochemical behaviour between various interfaces [32]. 3D image (0.79 × 0.79 µm) of scan of layer, formed by H7N7 virions is shown in Fig. 3B. It is obvious that H7N7 virion layer exhibit mainly positive relative current response of 30 nA. Positive current response is caused by the presence of influenza surface proteins, because HA proteins are positively charged in general [33,34]. This property is important for successful interaction with negatively charged membranes [35]. Considering the negatively charged surface of paramagnetic particles (approximately from -90 to -10 nA) as it is shown in Fig. 3C, this natural mechanism of virions forms strong charge-charge interaction with negatively charged composite´s surface. After establishment of binding (Fig. 3D), the relative current response still exhibits more positive values, when compared with bare composite (from -20 to 30 nA). Strong charge-charge interaction may be utilized for maintenance of specifity of PMPs-based isolation of influenza virions from matrixes, which contain substances charged weaker than influenza HA proteins. Because the isolation is based on charge, PMPs-based isolation may be applied only as a tool for rapid, screening diagnostics, but not for determination of various influenza subtypes, because all of them contain hemagglutinin in various amounts localized on lipid bilayer. On the other hand, influenza viruses replication is characterized by

a high mutation rate [36,37], complicating the biosensing, based on antisense oligonucleotides due to requirements for specific oligonucleotides sequences [38]. Hence, utilization of natural affinity based on different charges offers a tool for the isolation of uncharacterized influenza serotypes during epidemic or pandemic situations. Moreover many nanotechnology-based approaches such as gold nanoparticles [39], carbon nanotubes (CNTs) [40], quartz crystal microbalance (QCM) immunosensors [41], or silicon nanowires (SiNW) [42] may be enhanced by a pre-concentration step that it is often warranted when the virus level is very low. Paramagnetic particles synthesized by us may provide important, primary pre-concentration step before transduction of signal, and thus rapidly increase a sensitivity of biosensor.

4. CONCLUSION

In our study, we showed a preparation of nanomaghemite core, covered by outer silica shell formed by TEOS functionalized with APTES providing extra aminopropylsilane functional groups. Paramagnetic particles synthesized in this way exhibit perfect superparamagnetic and colloidal properties. Moreover, the resulting composite is able to establish a binding with H7N7 influenza virions, as it was confirmed by MALDI-TOF/TOF MS and scanning electrochemical microscopy. As it was identified, binding of virions and composite is based on strong charge-charge interaction, imitating the natural interaction between positively charged hemagglutinin and negatively charged cell membranes. Because the influenza virus is one of the most important infectious agents, and it is highly contagious, paramagnetic particles-based device may be applicable in rapid and cheap screening, throughout population in the form of biosensors or Lab-on-a-Chip platforms.

ACKNOWLEDGEMENTS

The authors acknowledge NanoBioMetalNet CZ.1.07/2.4.00/31.0023 for financial support. Moreover, the authors wish to express their thanks to Michal Zurek for perfect technical assistance.

Conflict of interest

The authors have declared no conflict of interest.

References

1. A. Jegerlehner, F. Zabel, A. Langer, K. Dietmeier, G. T. Jennings, P. Saudan and M. F. Bachmann, *PLoS One*, 8 (2013) 1.
2. J. K. Taubenberger, A. H. Reid, R. M. Lourens, R. X. Wang, G. Z. Jin and T. G. Fanning, *Nature*, 437 (2005) 889.
3. A. T. Cruz, A. C. Cazacu, J. M. Greer and G. J. Dernmler, *J. Clin. Virol.*, 41 (2008) 143.
4. A. Comin, N. Toft, A. Stegeman, D. Klinkenberg and S. Marangon, *Influenza Other Respir. Viruses*, 7 (2013) 257.
5. T. H. Jensen, G. Ajjouri, K. J. Handberg, M. J. Slomka, V. J. Coward, M. Cherbonnel, V. Jestin, P. Lind and P. H. Jorgensen, *Acta Vet. Scand.*, 55 (2013) 1.
6. Y. Y. Huang, M. Khan and Mandoiu, II, *PLoS One*, 8 (2013) 1.

7. A. Z. Hu, M. Colella, J. S. Tam, R. Rappaport and S. M. Cheng, *J. Clin. Microbiol.*, 41 (2003) 149.
8. M. Gueudin, A. Vabret, J. Petitjean, S. Gouarin, J. Brouard and F. Freymuth, *J. Virol. Methods*, 109 (2003) 39.
9. L. Krejcova, D. Hynek, V. Adam, J. Hubalek and R. Kizek, *Int. J. Electrochem. Sci.*, 7 (2012) 10779.
10. J. Wang, *Anal. Chim. Acta*, 469 (2002) 63.
11. S. O. Kelley, E. M. Boon, J. K. Barton, N. M. Jackson and M. G. Hill, *Nucleic Acids Res.*, 27 (1999) 4830.
12. V. Adam, D. Huska, J. Hubalek and R. Kizek, *Microfluid. Nanofluid.*, 8 (2010) 329.
13. G. Giakisikli and A. N. Anthemidis, *Talanta*, 110 (2013) 229.
14. P. F. Zong, S. F. Wang, Y. L. Zhao, H. Wang, H. Pan and C. H. He, *Chem. Eng. J.*, 220 (2013) 45.
15. A. A. Karamani, A. P. Douvalis and C. D. Stalikas, *J. Chromatogr. A*, 1271 (2013) 1.
16. J. de Jonge, J. M. Leenhouts, M. Holtrop, P. Schoen, P. Scherrer, P. R. Cullis, J. Wilschut and A. Huckriede, *Biochem. J.*, 405 (2007) 41.
17. O. Zitka, N. Cernei, Z. Heger, M. Matousek, P. Kopel, J. Kynicky, M. Masarik, R. Kizek and V. Adam, *Electrophoresis*, 34 (2013) 2639.
18. M. Enserink, *Science*, 324 (2009) 871.
19. Y. Zhang, Q. Y. Zhang, H. H. Kong, Y. P. Jiang, Y. W. Gao, G. H. Deng, J. Z. Shi, G. B. Tian, L. L. Liu, J. X. Liu, Y. T. Guan, Z. G. Bu and H. L. Chen, *Science*, 340 (2013) 1459.
20. D. Elton, E. A. Bruce, N. Bryant, H. M. Wise, S. MacRae, A. Rash, N. Smith, M. L. Turnbull, L. Medcalf, J. M. Daly and P. Digard, *Influenza Other Respir. Viruses*, 7 (2013) 81.
21. A. Cullinane and J. R. Newton, *Vet. Microbiol.*, 167 (2013) 205.
22. G. Sinigaglia, M. Magro, G. Miotto, S. Cardillo, E. Agostinelli, R. Zboril, E. Bidollari and F. Vianello, *Int. J. Nanomed.*, 7 (2012) 2249.
23. M. Magro, A. Faralli, D. Baratella, I. Bertipaglia, S. Giannetti, G. Salviulo, R. Zboril and F. Vianello, *Langmuir*, 28 (2012) 15392.
24. J. H. Min, M. K. Woo, H. Y. Yoon, J. W. Jang, J. H. Wu, C. S. Lim and Y. K. Kim, *Anal. Biochem.*, 447 (2014) 114.
25. R. Dominguez-Gonzalez, L. G. Varela and P. Bermejo-Barrera, *Talanta*, 118 (2014) 262.
26. C. M. J. Hu, R. H. Fang, B. T. Luk and L. F. Zhang, *Nanoscale*, 6 (2014) 65.
27. M. L. Reed, O. A. Bridges, P. Seiler, J. K. Kim, H. L. Yen, R. Salomon, E. A. Govorkova, R. G. Webster and C. J. Russell, *J. Virol.*, 84 (2010) 1527.
28. T. Suzuki, T. Takahashi, T. Saito, C. T. Guo, K. Hidar, D. Miyamoto and Y. Suzuki, *FEBS Lett.*, 557 (2004) 228.
29. T. Takahashi, T. Suzuki, K. Hidari, D. Miyamoto and Y. Suzuki, *FEBS Lett.*, 543 (2003) 71.
30. J. K. Xu, C. X. Ju, J. Sheng, F. Wang, Q. Zhang, G. L. Sun and M. Sun, *Bull. Korean Chem. Soc.*, 34 (2013) 2408.
31. J. Wang, *Biosens. Bioelectron.*, 21 (2006) 1887.

32. A. L. Barker, M. Gonsalves, J. V. Macpherson, C. J. Slevin and P. R. Unwin, *Anal. Chim. Acta*, 385 (1999) 223.
33. N. Arinaminpathy and B. Grenfell, *PLoS One*, 5 (2010) 1.
34. Y. Kobayashi and Y. Suzuki, *PLoS One*, 7 (2012) 1.
35. S. E. Hensley, S. R. Das, A. L. Bailey, L. M. Schmidt, H. D. Hickman, A. Jayaraman, K. Viswanathan, R. Raman, R. Sasisekharan, J. R. Bennink and J. W. Yewdell, *Science*, 326 (2009) 734.
36. G. Gabriel, V. Czudai-Matwich and H. D. Klenk, *Virus Res.*, 178 (2013) 53.
37. N. Liu, G. Y. Wang, K. C. Lee, Y. Guan, H. L. Chen and Z. W. Cai, *Faseb J.*, 23 (2009) 3377.
38. M. J. Lodes, D. Suciu, M. Elliott, A. G. Stover, M. Ross, M. Caraballo, K. Dix, J. Crye, R. J. Webby, W. J. Lyon, D. L. Danley and A. McShea, *J. Clin. Microbiol.*, 44 (2006) 1209.
39. J. D. Driskell, C. A. Jones, S. M. Tompkins and R. A. Tripp, *Analyst*, 136 (2011) 3083.
40. P. D. Tam, V. N. Hieu, N. D. Chien, A. T. Le and M. A. Tuan, *J. Immunol. Methods*, 350 (2009) 118.
41. D. J. Li, J. P. Wang, R. H. Wang, Y. B. Li, D. Abi-Ghanem, L. Berghman, B. Hargis and H. G. Lu, *Biosens. Bioelectron.*, 26 (2011) 4146.
42. E. Stern, J. F. Klemic, D. A. Routenberg, P. N. Wyrembak, D. B. Turner-Evans, A. D. Hamilton, D. A. LaVan, T. M. Fahmy and M. A. Reed, *Nature*, 445 (2007) 519.